

The nucleophilic addition of nitrones to carbonyl compounds: insights on the nature of the mechanism of the L-proline induced asymmetric reaction from a DFT analysis

Manuel Arnó, Ramón J. Zaragoza and Luis R. Domingo*

Instituto de Ciencia Molecular, Departamento de Química Orgánica, Universidad de Valencia, Dr. Moliner 50, E-46100 Burjassot, Valencia, Spain

Received 17 February 2004; accepted 16 March 2004

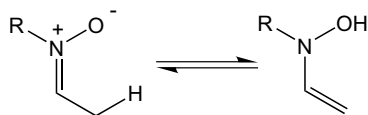
Abstract—The mechanism of the L-proline induced asymmetric nitron–aldol reaction of *N*-methyl-*C*-ethylnitron with dimethyl ketomalonate has been studied by using density functional theory at B3LYP/6-31G** level. The reaction was initialized by the addition of L-proline to the nitron to form an aminal, which by elimination of the hydroxylamine gave a chiral enamine. The nucleophilic addition of this chiral enamine to dimethyl ketomalonate corresponds to stereoselective C–C bond-formation step. Further nucleophilic addition of hydroxylamine to the zwitterionic intermediate formed in the enamine addition gave a second aminal, which by L-proline elimination afforded the corresponding β -hydroxynitron. The B3LYP/6-31G** results are in acceptable agreement with previous experiments, allowing us to explain the stereoselectivity on the C–C bond-formation step.

© 2004 Elsevier Ltd. All rights reserved.

1. Introduction

Nitrones are important compounds in organic synthesis as they are known to undergo two fundamental reactions: 1,3-dipolar cycloadditions with alkenes,^{1,2} and addition of nucleophiles.³ Recently, Jorgensen et al.⁴ reported a new and interesting reaction of nitrones. This is a new C–C bond-formation process in which the nitron acts as a nucleophile that adds to activated electrophiles such as carbonyl compounds.

Nitrones with an α -hydrogen are in equilibrium with the hydroxylamine tautomer (see Scheme 1). The latter possesses a nucleophilic carbon atom, which can add to activated carbonyl compounds. This reaction can be considered as the nitron analogue of the aldol reaction,

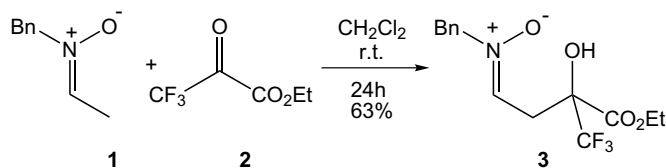


Scheme 1.

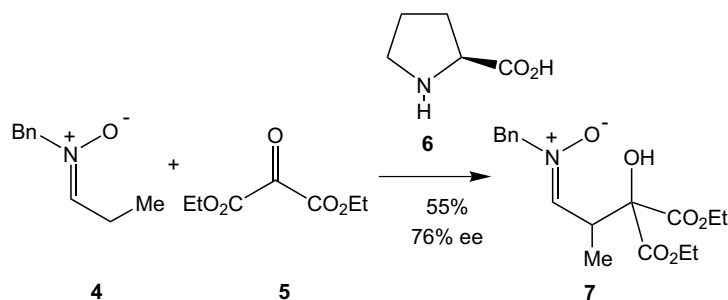
that is, a *nitron–aldol reaction*. Thus, *N*-benzyl-*C*-methylnitron **1** with an α -hydrogen in a primary carbon atom reacts with ethyl 1,1,1-trifluoropyruvate **2** to give β -hydroxynitron **3** in 63% yield (see Scheme 2).⁴ The use of Broensted and Lewis acids as catalysts did not improve the reaction rate significantly. However, the presence of a secondary cyclic amine such as pyrrolidine led to a significant enhancement of the reaction rate. Jorgensen et al. investigated further the reactions of a series of α -substituted nitrones with diethyl ketomalonate **5** in presence of L-proline **6** as a chiral catalyst and found an improvement in enantioselectivity.⁴ Thus, the *N*-benzyl nitron derivative **4** from propionaldehyde reacts with diethyl ketomalonate **5** to give the β -hydroxynitron **7** in 55% isolated yield and with 76% ee (see Scheme 3).

Based upon a series of investigations, Jorgensen et al.⁴ proposed for the enantioselective L-proline catalyzed process the mechanism given in Scheme 4. The first step is the nucleophilic addition of L-proline **6** to nitron **4** to form the aminal **8**, which upon elimination of benzylhydroxylamine **9** gave chiral enamine **10**. The authors proposed that the enantioselectivity was induced by the addition of **10** to carbonyl compound **5**. The zwitterionic adduct **11** then reacts with **9** to form a second aminal **12** from which L-proline is eliminated and the nonracemic β -hydroxynitron **7** obtained.

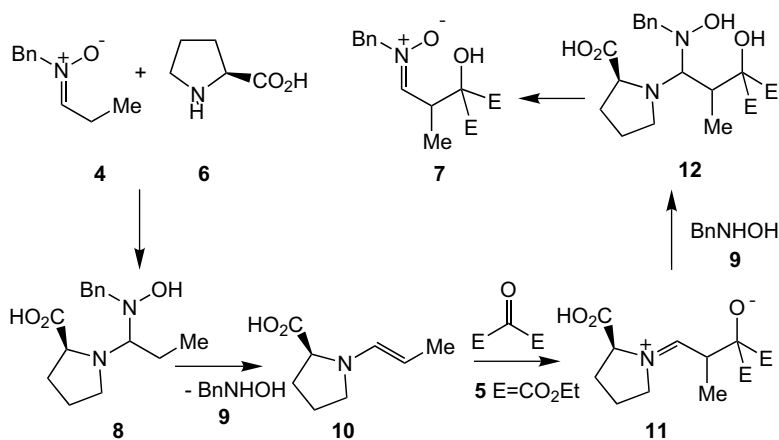
* Corresponding author. Tel.: +34-96-354-3106; fax: +34-96-354-3152; e-mail: domingo@utopia.uv.es



Scheme 2.



Scheme 3.

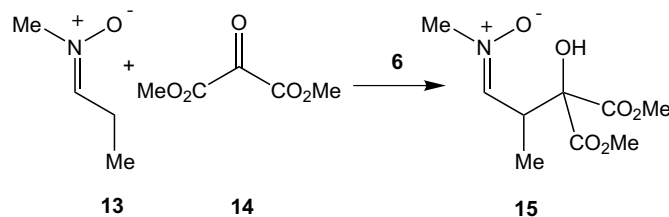


Scheme 4.

Our interest in enzymatic-type catalyzed aldol reactions⁵ prompted us to carry out a theoretical investigation on the mechanism of the L-proline catalyzed intermolecular aldol reaction.⁶ In view of the significance of L-proline in bioorganic catalyzed processes we herein report the mechanism for the L-proline induced asymmetric nitron-aldol reaction, studied recently experimentally by Jorgensen et al.⁴ using density functional theory (DFT) with the well-established B3LYP/6-31G** method. The reactions between *N*-methyl-*C*-ethylnitron **13** and dimethyl ketomalonate **14** in the absence or presence of L-proline **6** to yield β -hydroxynitron **15** have been selected as computational models (see Scheme 5). The stereoselectivity for the C–C bond-formation step can be analyzed through the nucleophilic attack of the chiral enamine **10** to **14**. Furthermore, the role of the acid carboxylate group present on the L-proline catalyst in the mechanism will be examined.

2. Computational methods

Density functional theory⁷ calculations have been carried out using the B3LYP⁸ exchange-correlation functions, together with the standard 6-31G** basis set.⁹ An exhaustive exploration of the potential energy surfaces (PESs) was carried out to ensure that all relevant stationary points were located and properly characterized. Optimizations were carried out using the Berny analytical gradient optimization method.¹⁰ The stationary points were characterized by frequency calculations in order to verify that minima and transition structures have zero and one imaginary frequency, respectively.¹¹ The intrinsic reaction coordinate (IRC)¹² paths were traced in order to verify the energy profiles connecting each transition structure to the two associated minima of the proposed mechanism by using the second order González–Schlegel integration method.¹³ The electronic



Scheme 5.

structures of the stationary points were analyzed by the natural bond orbital (NBO) method.¹⁴ All calculations were carried out with the GAUSSIAN 98 suite of programs.¹⁵ Optimized geometries of all stationary points on PES are available from the authors.

Recent studies carried out for related reactions show that the geometry optimization of the stationary points on PES, while taking into account the solvent effects via a continuum model, does not substantially modify the gas phase geometries.⁶ Therefore, the solvent effects have been considered by single point calculations at the B3LYP/6-31G** gas phase stationary points using a relatively simple self-consistent reaction field (SCRF) method¹⁶ based on the polarizable continuum model (PCM) of Tomasi and co-workers.¹⁷ The solvent used in the experimental work was dichloromethane and as a result, we used its dielectric constant $\epsilon = 8.93$.

3. Results and discussion

First, the nucleophilic attack of the hydroxylenamine tautomer **16** of the *N*-methyl-*C*-ethylnitronium **13** to dimethyl ketomalonate **14** will be discussed. Then, the mechanism of the *L*-proline promoted asymmetric nitronium–aldol reaction between **13** and **14** will be analyzed.

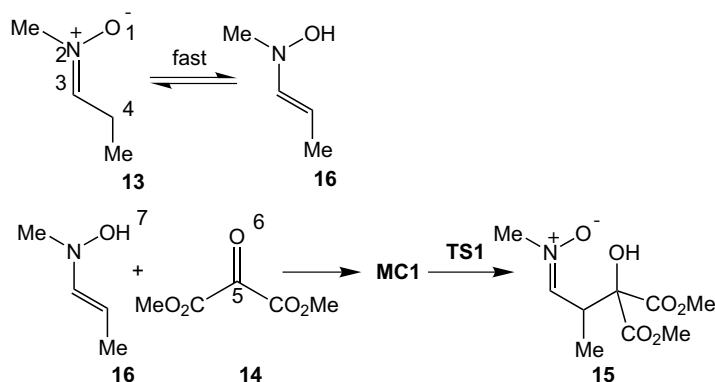
3.1. Nucleophilic attack of the hydroxylenamine **16** to dimethyl ketomalonate **14**

The nitronium–aldol reaction between nitronium **13** and ketodiester **14** is a stepwise process. The first step involves the tautomerization of nitronium **13** to hydroxy-

enamine **16**, while the second step is the nucleophilic attack of **16** to dimethyl ketomalonate **14** (see Scheme 6). In Table 1 the total energies of the stationary points for the nitronium–aldol reaction between **13** and **14** in vacuo and in dichloromethane are given, while the geometry of the TS is shown in Figure 1. Since some

Table 1. B3LYP/6-31G** total energies (in a.u.) of the stationary points involved in the nitronium–aldol-type reaction between of *N*-methyl-*C*-ethylnitronium **13** and dimethyl ketomalonate **14** in the absence and presence of *L*-proline **6**, in vacuum and in dichloromethane

	In vacuum	In dichloromethane
13	−287.761880	−287.766936
16	−287.749965	−287.753446
14	−570.250272	−570.255748
MC1	−858.009934	−858.015511
TS1	−858.000182	−858.008583
(<i>R</i>)- 15	−858.040204	−858.048492
6	−401.166580	−401.173612
MC2	−688.953726	−688.960658
TS2	−688.921526	−688.935455
17	−688.934927	−688.949229
18	−688.943990	−688.951408
TS3	−688.910266	−688.926141
10	−171.030512	−171.034335
20	−517.870718	−517.889314
TS4	−517.856072	−517.869599
10	−517.888189	−517.894831
MC3	−1088.150631	−1088.160084
(<i>R</i>)- TS5	−1088.141657	−1088.155436
(<i>S</i>)- TS5	−1088.133859	−1088.144896
(<i>R</i>)- 21	−1088.154431	−1088.171216
(<i>S</i>)- 21	−1088.151963	−1088.167615
TS6	−1259.174053	−1259.192534
(<i>RS</i>)- 22	−1259.208271	−1259.219749
(<i>RS</i>)- 23	−1259.190217	−1259.208621
TS7	−1259.188532	−1259.203179



Scheme 6.

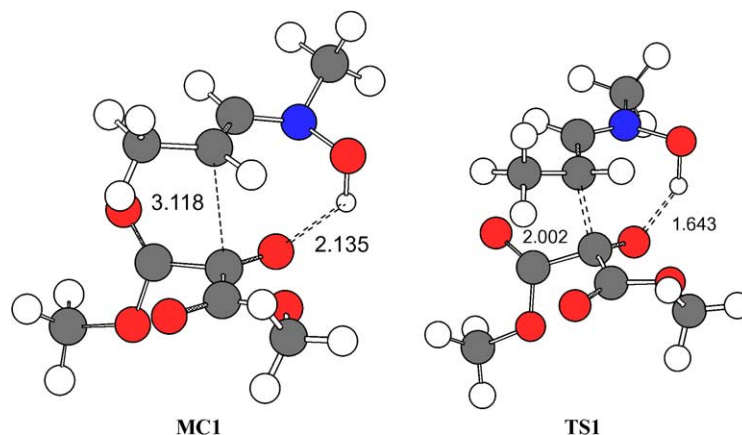


Figure 1. Geometries of the molecular complex **MC1** and the transition structure **TS1** involved in the nucleophilic attack of hydroxylenamine **16** to dimethyl ketomalonate **14**. The bond lengths directly involved in the reaction are given in angstroms.

pathways involve zwitterionic intermediates, and solvent effects can stabilize these species, the energetic discussion will be performed using the energies obtained in dichloromethane.

Jorgensen and co-workers found that in the absence of a secondary amine catalyst the rate of formation of the adduct had a first order dependency of the concentration of nitron and carbonyl compound.⁴ This indicates that the first step is a fast equilibration between nitron **13** and tautomer **16**. The latter is 8.5 kcal/mol higher in energy than nitron **13**.

The second step in the nucleophilic attack of hydroxylenamine **16** to the dimethyl ketomalonate **14** gives β -hydroxynitron **15**, via **TS1**. The IRC analysis from **TS1** to reactants allows us to find a molecular complex (MC), **MC1**, in which the carbonyl oxygen atom of the ketodiester **14** is hydrogen bonded to the hydroxylenamine **16** through the H7 hydrogen atom (see Scheme 6 and Fig. 1). **MC1** is 4.4 kcal/mol lower in energy than the separated reactants as a consequence of hydrogen-bond formation. This hydrogen-bond favors the subsequent C–C bond-formation step through a stabilization of the negative charge that is located at the carbonyl oxygen atom of **14** along the nucleophilic attack of hydroxylenamine **16**.^{6,18} Additionally, this hydrogen-bond allows the proton transfer process in a concerted fashion. The activation barrier for the C–C bond-formation step from the separated reagents **13** and **14** is 8.8 kcal/mol. The IRC analysis from **TS1** to adduct **15** shows that after the TS the C–C bond-formation and the proton transfer processes are concerted. The formation of the β -hydroxynitron **16** was exothermic by 16.2 kcal/mol.

At **MC1** the distance between the H7 hydrogen and the O6 oxygen atoms was 2.135 Å, whilst the distance between the C4 and C5 carbon atoms that were bonded was 3.118 Å (see Fig. 1). At **TS1** the length of the C4–C5 forming bond was 2.002 Å, while the distance between the H7 hydrogen and the O6 oxygen atoms was 1.643 Å.

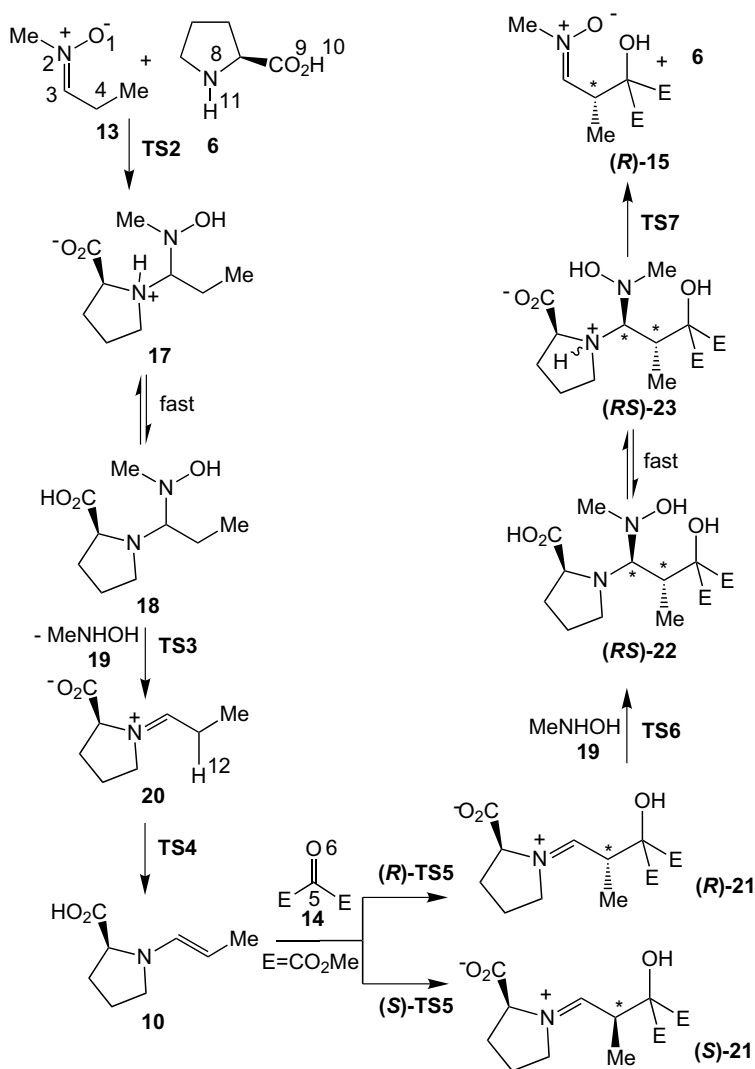
The extent of the bond-formation along a reaction pathway was provided by the concept of bond order (BO).¹⁹ The BO of the C4–C5 forming bond at **TS1** was 0.49, while the BO values between the H7 hydrogen atom and the O1 and O6 oxygen atoms were 0.59 and 0.11, respectively. These data indicate that at **TS1** the C4–C5 bond-formation is more advanced than the proton transfer process.

3.2. L-Proline promoted asymmetric nitron–aldol reaction between nitron **13** and dimethyl ketomalonate **14**

The L-proline promoted asymmetric nitron–aldol reaction between nitron **13** and dimethyl ketomalonate **14** has a complex mechanism that is summarized in the Scheme 7. The total energies of the stationary points are given in Table 1, while the geometries of the TSs are shown in Figure 2.

The first step is the addition of L-proline **6** to nitron **13** to give the zwitterionic intermediate **17**, which equilibrates with amina **18** (see Scheme 7). The IRC analysis from **TS2** to reactants allows us to find a MC, **MC2**, in which the O1 oxygen atom of the nitron **13** is hydrogen bonded to L-proline **6** through its acidic H10 hydrogen atom. **MC2** is 12.6 kcal/mol lower in energy than the separated reactants as a consequence of the hydrogen-bond formation. This hydrogen-bond catalyzes the C–N bond-formation process through an enhancement of the electrophilicity of **13**. The activation barrier for the nucleophilic attack of L-proline **6** to the nitron **13**, via **TS2**, was 15.8 kcal/mol from **MC2** (3.2 kcal/mol from **13** and **6**). The zwitterionic intermediate **17** via an acid/base process equilibrates with the amina **18**. The addition of L-proline **6** to the nitron **13** to give the amina **18** was exothermic by 6.8 kcal/mol.

The next process was the elimination of methylhydroxylamine **19** on amina **18** to give the zwitterionic intermediate **20** via **TS3** (see Scheme 7). Experiments carried out by Jorgensen and co-workers in which different substituted nitrones interchange the *N*-alkyl



Scheme 7.

groups along the L-proline catalyzed process support this hydroxylamine elimination.⁴ The activation barrier for the methylhydroxylamine elimination via **TS3** was 15.9 kcal/mol. The conversion of the zwitterionic intermediate **20** into the enamine **10** took place via an intramolecular proton abstraction by the carboxylate residue present in **20**, via **TS4**. The activation barrier for this intramolecular process was 12.4 kcal/mol. The transformation of aminal **18** into enamine **10** plus hydroxylamine **19** was endothermic by ca. 14 kcal/mol. This elimination is entropically favored.

The next step corresponded to the nucleophilic attack of chiral enamine **10** to the carbonyl C5 carbon atom of dimethyl ketomalonate **14**. For this process that corresponds to the C–C bond-formation step, two diastereoisomeric reactive channels are feasible (see Scheme 7) They correspond to the approach of carbonyl derivative **14** to the two prochiral faces of the enamine **10**. Therefore, this is the stereoselectivity determining-step of the L-prolines catalyzed process.

An analysis of the PES for this process allowed us to find several MCs in which the carbonyl O6 oxygen atom of the ketodiester **14** is hydrogen-bonded to the L-proline residue of **10** through the acidic H10 hydrogen atom. The more stable one, **MC3**, was ca. 6.0 kcal/mol lower in energy than the separated reactants as a consequence of the hydrogen-bond formation. This hydrogen-bond catalyzed the C–C bond-formation process by an enhancement of the electrophilicity of ketodiester **14**. A similar acid catalysis has been found on the L-proline catalyzed aldol reaction.^{6,18} The B3LYP/6-31G** activation barriers associated to (*R*)-**TS5** and (*S*)-**TS5** relative to the more stable MC, (*R*)-**MC3**, were 2.9 and 9.5 kcal/mol, respectively. These results indicate that the attack of the dimethyl ketomalonate **14** along the *re* face of the chiral enamine **10**, yielding (*R*)-**21**, is clearly favored relative to the attack along the *si* face. These energetic results are in reasonable agreement with stereochemical outcome observed in the reaction between the nitrone **4** and ketomalonate **5** in the presence of L-proline **6**.⁴ The C–C bond-formation step was exothermic by 13 kcal/mol.

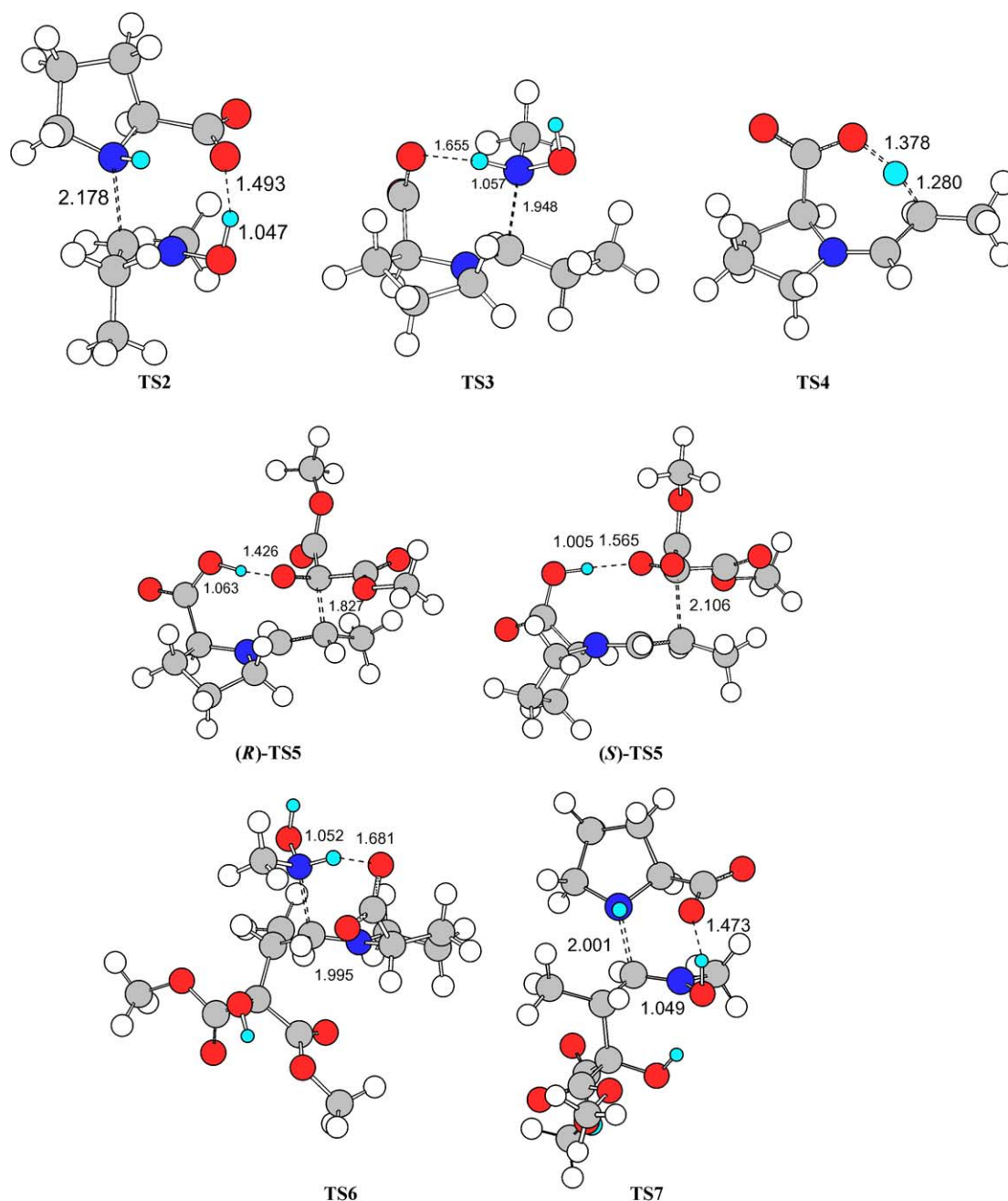


Figure 2. Geometries of the transition structures involved in the L-proline promoted asymmetric nitrene-aldol reaction between **13** and **14**. The bond lengths directly involved in the reaction are given in angstroms.

The next step involved the nucleophilic addition of methylhydroxylamine **19** to the zwitterionic intermediate (*R*)-**21** (see Scheme 7). This addition took place at both prochiral faces of the iminium framework of (*R*)-**21** to give a pair of diastereoisomeric aminals. However, the subsequent L-proline elimination only yielded the β -hydroxynitrone (*R*)-**15** as a consequence of the loss of stereochemistry at the C3 carbon atom. We only considered the addition of **19** to (*R*)-**21** through the *si* face because it allows the concerted hydrogen transfer from the hydroxylamine to the carboxylate. The activation barrier for the addition of hydroxylamine **19** to (*R*)-**21** via **TS6** was 8.2 kcal/mol, being the process exothermic by 8.9 kcal/mol.

Finally, the last step was the L-proline elimination to give the β -hydroxynitrone adducts (*R*)-**15**. This step required the initial equilibration between the aminal (*RS*)-**22** and the zwitterionic intermediate (*RS*)-**23** (see Scheme 7). This isomerization was endothermic by 7.0 kcal/mol; however, formation of (*RS*)-**23** favored the subsequent L-proline elimination by: (i) the formation of an ammonium cation that assists the C3–N8 breaking-bond process; and (ii) the hydrogen-bond formation between the H10 hydrogen and the O9 oxygen atoms that allows the formation of two neutral molecules in a concerted fashion. As a result, this elimination presents a very low activation barrier, 3.4 kcal/mol, with the

process being exothermic by 8.5 kcal/mol. The overall process was exothermic by 16.2 kcal/mol.

The geometries of the TSs associated with the L-proline induced asymmetric nitron–aldol reaction are given in Figure 2. At the TS associated with the nucleophilic addition of L-proline **6** to the nitron **13**, **TS2**, the length of the C3–N8 forming bond was 2.178 Å. The BO value of the forming bond was 0.31, while the BO values between the H10 hydrogen atom and the O9 and the O1 oxygen atoms were 0.18 and 0.53, respectively. These BOs indicate that at this TS the proton transfer is very advanced. At the TS associated with the elimination of hydroxylamine, **TS3**, the length of C3–N2 breaking bond was 1.948 Å, while the BO value was 0.47. At this TS, the BO values between the H10 hydrogen atom and carboxyl O9 oxygen and nitron N2 nitrogen atoms were 0.11 and 0.64, respectively. These BOs indicate that at the TS, the proton transfer process is more advanced than the C3–N2 breaking bond one. At the TS associated with the intramolecular proton transfer at the zwitterionic intermediate **20**, **TS4**, the lengths of the C4–H12 breaking and O9–H12 forming bonds were 1.280 and 1.378 Å, respectively. The BOs of these breaking and forming bonds were 0.50 and 0.26, respectively.

At the two diastereoisomeric TSs associated with the C–C bond-formation step, (*R*)-**TS5** and (*S*)-**TS5**, the lengths of the C4–C5 forming bond were 1.827 and 2.106 Å, while the BOs were 0.64 and 0.40, respectively. The more favorable (*R*)-**TS5** is more advanced than (*S*)-**TS5**. The BO values between the H10 atom and the carbonyl O6 oxygen atom at these TSs were 0.22 and 0.13, while the O9–H10 BOs were 0.55 and 0.58, respectively. These BO values point to a strong hydrogen-bond that catalyzes the C–C bond-formation.^{6,18}

At the TS associated with the nucleophilic attack of the hydroxylamine **19** to the zwitterionic intermediate (*R*)-**21**, **TS6**, the length of the C3–N2 forming bond was 1.995 Å. The BO of the C3–N2 forming bond was 0.43, while the BO values between the H10 hydrogen and the N2 nitrogen and the O9 oxygen atoms were 0.66 and 0.10, respectively. These values indicate that the H10

hydrogen atom is not being transferred at this TS. At the TS associated with the L-proline elimination, **TS7**, the length of the C3–N8 breaking bond was 2.001 Å. The BO of the C3–N8 breaking bond was 0.44, while the BO values between the H10 hydrogen and the O1 and O9 oxygen atoms were 0.51 and 0.18, respectively. These data indicate that the C2–N8 breaking bond is more advanced than the H10 proton transfer one. The analysis of BO values at the TSs involved in the L-proline induced asymmetric reaction indicates that the acid carboxylic group of L-proline participates catalyzing the most of the steps of this hard mechanism.

Finally, in order to explain the origin of the diastereoselection in the L-proline induced asymmetric reaction, the TSs involved at the stereoselective determining-step, (*R*)-**TS5** and (*S*)-**TS5**, were geometrically and electronically analyzed. A first conformational analysis along the C4–C5 forming bond at these TSs showed a similar rearrangement of ketodiester **14** relative to chiral enamine **10** as a consequence of the symmetry present on the former (see Fig. 3).

The natural population analysis¹⁴ allowed us to evaluate the charge transfer along the C4–C5 bond-formation process. The natural charges at these diastereoisomeric TSs were shared between the donor enamine **10** and the acceptor ketodiester **14**. The charge transferred from **10** to **14** at the two TSs were: 0.52 e at (*R*)-**TS5** and 0.37 e at (*S*)-**TS5**. These values indicate that these TSs have some zwitterionic character that is larger at the more favorable (*R*)-**TS5**. This analysis is in agreement with the larger dipole moment of (*R*)-**TS5**, 6.89 D, than (*S*)-**TS5**, 4.81 D (see Fig. 3). Two factors contribute to the large charge transfer at the more favorable (*R*)-**TS5**: (i) a stronger hydrogen-bond formation at (*R*)-**TS5** than at (*S*)-**TS5**: the length of the hydrogen-bond between the H10 hydrogen and the carbonyl O6 oxygen atoms at (*R*)-**TS5**, 1.426 Å, is shorter than that at (*S*)-**TS5**, 1.565 Å; and (ii) a larger coulombic interaction between the ends of the zwitterionic (*R*)-**TS5** than at (*S*)-**TS5**: the distance between the positively charged N8 nitrogen atom and the negatively charged carbonyl O6 oxygen atom at (*R*)-**TS5**, 2.690 Å, is shorter than that at

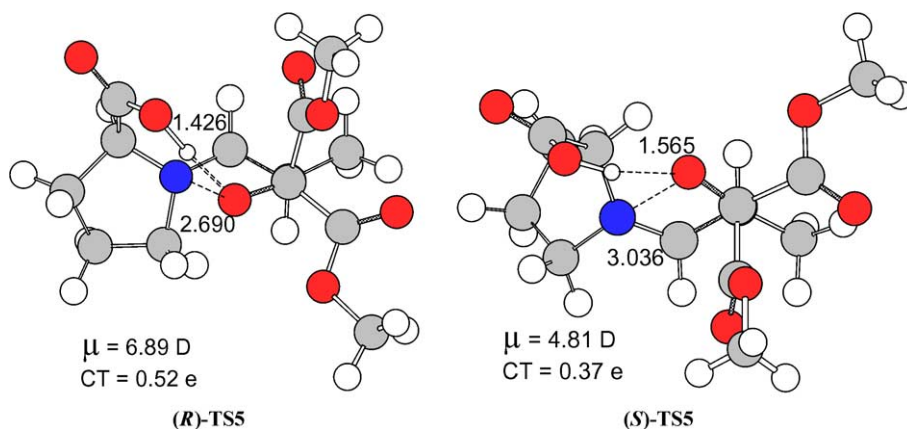


Figure 3. Geometries of the diastereoisomeric (*R*)-**TS5** and (*S*)-**TS5** viewed along the C5–C6 forming bond. The H10–O6 and O6–N8 distances are given in angstroms. The dipole moments, μ in D, and the charge transfer, CT in e, are also given.

(*S*)-TS5, 3.036 Å. Both factors increase the electrophilicity of the acceptor carbonyl group along the *re face* approach and, as a consequence, the *re* channel is favored over the *si* one.

4. Conclusions

The mechanisms for the nitron–aldol reaction of *N*-methyl-*C*-ethylnitron with dimethyl ketomalonate in the absence or presence of *L*-proline have been studied by using density functional theory (DFT) at B3LYP/6-31G** level. In the absence of *L*-proline, the nitron–aldol reaction had a stepwise mechanism that was initialized by the fast tautomerization of the *C*-ethylnitron. The second process was the nucleophilic attack of the hydroxylamine form to dimethyl ketomalonate. This process, which corresponds to the C–C bond-formation step, is catalyzed by an intramolecular hydrogen-bond between the hydroxylic hydrogen atom of the hydroxylamine and the carbonyl oxygen atom of the ketodiester that enhances the electrophilicity of the carbonyl acceptor.

In the presence of *L*-proline the nitron–aldol reaction presented a more complex mechanism. The first step involved the addition of *L*-proline to the nitron to form an aminal, which by elimination of the hydroxylamine gave a chiral enamine. The nucleophilic addition of this chiral enamine to dimethyl ketomalonate corresponds to the stereoselective C–C bond-formation step. Further nucleophilic addition of hydroxylamine to the zwitterionic intermediate formed in the enamine addition gave a second aminal, which by *L*-proline elimination afforded the corresponding β -hydroxynitron. The analysis of BO values at the TSs involved in the *L*-proline induced asymmetric reaction indicated that the carboxylic acid group of *L*-proline participated in catalyzing most of the steps of this hard mechanism.

The B3LYP/6-31G** calculations show that the electrophilic attack of the ketodiester through the *re face* of the chiral enamine is favored by a stronger hydrogen-bond formation and larger coulombic interactions between the ends of the zwitterionic TS than those associated with the *si face* approach. These factors contribute to an enhancement of the electrophilicity of the acceptor carbonyl compound along the *re* approach, this being the more favorable channel. These results are in reasonable agreement with previous experiments, allowing us to explain the stereoselectivity on the C–C bond-formation step.

Acknowledgements

This work was supported by research funds provided by the Ministerio de Educación y Cultura of the Spanish Government by DGICYT (project BQU2002-01032), and by the Agencia Valenciana de Ciencia y Tecnología of the Generalitat Valenciana (reference GRUPOS03/176).

References and notes

- (a) Huisgen, R. In *1,3-Dipolar Cycloaddition Chemistry*; Padwa, A., Ed.; Wiley: New York, 1984; Vol. 1, p 1; (b) Tufariello, J. J. In *1,3-Dipolar Cycloaddition Chemistry*; Padwa, A., Ed.; Wiley: New York, 1984; Vol. 2, p 83; (c) Torrsell, K. B. G. *Nitrile Oxides, Nitrones and Nitronates in Organic Synthesis*; VCH: New York, 1988; (d) *The Chemistry of Heterocyclic Compounds 59: Synthetic Applications of 1,3-Dipolar Cycloaddition Reactions towards Heterocycles and Natural Product*; Padwa, A., Pearson, W., Eds.; Wiley: New York, 2002.
- (a) Gothelf, K. V.; Jorgensen, K. A. *Chem. Rev.* **1998**, *98*, 863–909; (b) Gothelf, K. V.; Jorgensen, K. A. *Chem. Commun.* **2000**, 1449–1458; (c) Frederickson, M. *Tetrahedron* **1997**, *53*, 403–425; (d) Karlsson, S.; Höberg, H.-E. *Org. Prep. Proc. Int.* **2001**, *33*, 105–172.
- (a) Lombardo, M.; Trombini, C. *Synthesis* **2000**, 759–774; (b) Merino, P.; Franco, S.; Merchan, F. L.; Tejero, T. *Synlett* **2000**, 442–454.
- Bogevig, A.; Gothelf, K. V.; Jorgensen, K. A. *Chem. Eur. J.* **2002**, *8*, 5652–5661.
- (a) Arnó, M.; Domingo, L. R. *Int. J. Quant. Chem.* **2001**, *83*, 338–347; (b) Arnó, M.; Domingo, L. R. *Org. Biomol. Chem.* **2003**, *1*, 637–643.
- Arnó, M.; Domingo, L. R. *Theor. Chem. Acc.* **2002**, *108*, 232–239.
- (a) Parr, R. G.; Yang, W. *Density Functional Theory of Atoms and Molecules*; Oxford University Press: New York, 1989; (b) Ziegler, T. *Chem. Rev.* **1991**, *91*, 651–667.
- (a) Becke, A. D. *J. Chem. Phys.* **1993**, *98*, 5648–5652; (b) Lee, C.; Yang, W.; Parr, R. G. *Phys. Rev. B* **1988**, *37*, 785–789.
- Hehre, W. J.; Radom, L.; Schleyer, P. v. R.; Pople, J. A. *Ab initio Molecular Orbital Theory*; Wiley: New York, 1986.
- (a) Schlegel, H. B. *J. Comput. Chem.* **1982**, *3*, 214–218; (b) Schlegel, H. B. Geometry Optimization on Potential Energy Surface. In *Modern Electronic Structure Theory*; Yarkony, D. R., Ed.; World Scientific Publishing: Singapore, 1994.
- Tapia, O.; Andrés, J. *Chem. Phys. Lett.* **1984**, *109*, 471–477.
- Fukui, K. *J. Phys. Chem.* **1970**, *74*, 4161–4163.
- (a) González, C.; Schlegel, H. B. *J. Phys. Chem.* **1990**, *94*, 5523–5527; (b) González, C.; Schlegel, H. B. *J. Chem. Phys.* **1991**, *95*, 5853–5860.
- (a) Reed, A. E.; Weinstock, R. B.; Weinhold, F. *J. Chem. Phys.* **1985**, *83*, 735–746; (b) Reed, A. E.; Curtiss, L. A.; Weinhold, F. *Chem. Rev.* **1988**, *88*, 899–926.
- Frisch, M. J.; Trucks, G. W.; Schlegel, H. B.; Scuseria, G. E.; Robb, M. A.; Cheeseman, J. R.; Zakrzewski, V. G.; Montgomery, J. J. A.; Stratmann, R. E.; Burant, J. C.; Dapprich, S.; Millam, J. M.; Daniels, A. D.; Kudin, K. N.; Strain, M. C.; Farkas, O.; Tomasi, J.; Barone, V.; Cossi, M.; Cammi, R.; Mennucci, B.; Pomelli, C.; Adamo, C.; Clifford, S.; Ochterski, J.; Petersson, G. A.; Ayala, P. Y.; Cui, Q.; Morokuma, K.; Malick, D. K.; Rabuck, A. D.; Raghavachari, K.; Foresman, J. B.; Cioslowski, J.; Ortiz, J. V.; Stefanov, B. B.; Liu, G.; Liashenko, A.; Piskorz, P.; Komaromi, I.; Gomperts, R.; Martin, R. L.; Fox, D. J.; Keith, T.; Al-Laham, M. A.; Peng, C. Y.; Nanayakkara, A.; Challacombe, M.; W. Gill, P. M.; Johnson, B.; Chen, W.; Wong, M. W.; Andres, J. L.; Gonzalez, C.; Head-Gordon, M.; Replogle, E. S.; Pople, J. A. GAUSSIAN 98, Revision A.6 Gaussian, Inc.: Pittsburgh, PA, 1998.
- (a) Tapia, O. *J. Math. Chem.* **1992**, *10*, 139–181; (b) Tomasi, J.; Persico, M. *Chem. Rev.* **1994**, *94*, 2027–2094; (c) Simkin, B. Y.; Sheikhet, I. *Quantum Chemical and Statistical Theory of Solutions—A Computational Approach*; Ellis Horwood: London, 1995.

17. (a) Cances, E.; Mennunci, B.; Tomasi, J. *J. Chem. Phys.* **1997**, *107*, 3032–3041; (b) Cossi, M.; Barone, V.; Cammi, R.; Tomasi, J. *Chem. Phys. Lett.* **1996**, *255*, 327–335; (c) Barone, V.; Cossi, M.; Tomasi, J. *J. Comput. Chem.* **1998**, *19*, 404–417.
18. (a) Bahmanyar, S.; Houk, K. N. *J. Am. Chem. Soc.* **2001**, *123*, 12911–12912; (b) Bahmanyar, S.; Houk, K. N.; Martin, H. J.; List, B. *J. Am. Chem. Soc.* **2003**, *125*, 2475–2479.
19. Wiberg, K. B. *Tetrahedron* **1968**, *24*, 1083–1096.